

Prognostic Significance of ^{18}F -FDG PET Parameters and Plasma Epstein-Barr Virus DNA Load in Patients with Nasopharyngeal Carcinoma

Kai-Ping Chang¹, Ngan-Ming Tsang², Chun-Ta Liao¹, Cheng-Lung Hsu³, Ming-Jui Chung⁴, Chuan-Wei Lo⁴, Sheng-Chieh Chan⁴, Shu-Hang Ng⁵, Hung-Ming Wang³, and Tzu-Chen Yen⁴

¹Department of Otolaryngology–Head and Neck Surgery, Chang Gung Memorial Hospital and Chang Gung University College of Medicine, Taipei, Taiwan; ²Department of Radiation Oncology, Chang Gung Memorial Hospital and Chang Gung University College of Medicine, Taipei, Taiwan; ³Division of Hematology and Oncology, Department of Internal Medicine, Chang Gung Memorial Hospital and Chang Gung University College of Medicine, Taipei, Taiwan; ⁴Department of Nuclear Medicine and Molecular Imaging Center, Chang Gung Memorial Hospital and Chang Gung University College of Medicine, Taipei, Taiwan; and ⁵Department of Diagnostic Radiology, Chang Gung Memorial Hospital and Chang Gung University College of Medicine, Taipei, Taiwan

The plasma concentration of Epstein-Barr virus (EBV) DNA is associated with tumor burden and prognosis in patients with nasopharyngeal carcinoma (NPC), but data on the relationship between viral load and ^{18}F -FDG PET functional parameters are lacking. We examined the association of ^{18}F -FDG PET functional parameters and EBV DNA load with the clinicopathologic characteristics and clinical outcomes of patients with NPC.

Methods: One hundred eight patients with NPC who underwent ^{18}F -FDG PET before treatment were included in this study. We determined total lesion glycolysis (TLG) of the primary tumor, the cervical nodes, and their combination and the maximal standardized uptake value of the primary tumor and cervical lymph nodes. EBV DNA was measured by real-time polymerase chain reaction. **Results:** EBV DNA was significantly associated with total TLG ($R^2 = 0.589$). Total TLG values had the highest correlation with EBV DNA load and were significantly associated with tumor, nodal, and overall stages. However, tumor TLG greater than the median (>65 g) was the only parameter significantly associated with overall, local recurrence-free, disease-free, and distant metastasis-free survivals ($P = 0.033$, 0.014 , <0.001 , and 0.023 , respectively). After allowance for potential confounders, tumor TLG retained its independent significance for overall and disease-free survival rates ($P = 0.045$ and 0.006 , respectively). **Conclusion:** Total TLG values are primarily associated with tumor burden and clinical stage, whereas tumor TLG is the best predictor of patient survival after treatment.

Key Words: nasopharyngeal carcinoma; EBV; FDG PET; total lesion glycolysis; metabolic tumor volume

J Nucl Med 2012; 53:21–28

DOI: 10.2967/jnumed.111.090696

Nasopharyngeal carcinoma (NPC) is one of the most common types of head and neck cancer in Southeast Asia. NPC is a very radiosensitive tumor, and 5-y overall survival (OS) and disease-free survival (DFS) rates of up to 70% can be obtained by the use of concurrent chemoradiotherapy (1–3). However, some patients may still develop locoregional and distant failure, thus requiring salvage or palliative therapy (4–6). For these reasons, the development of more tailored treatment approaches can ultimately improve clinical outcomes.

The recognition of the importance of Epstein-Barr virus (EBV) in the pathogenesis of NPC (7–9) has stimulated a growing interest in EBV-based biomarkers for patients with this malignancy (10,11). Notably, the assessment of cell-free EBV DNA load may not only serve for detection of NPC (11) but also have value for prediction of prognosis and treatment outcomes. For instance, it has been reported that posttreatment EBV DNA levels may be clinically useful for monitoring tumor relapse (11–13).

Several investigators have examined the value of ^{18}F -FDG PET functional parameters for treatment planning in different malignancies, including NPC (14–16). A novel functional parameter—termed total lesion glycolysis (TLG) and defined as the standardized uptake value (SUV) multiplied by metabolic tumor volume (MTV)—has been described previously (17). TLG integrates both anatomic and biologic data and has been shown to predict prognosis in breast, colorectal, and lung cancers (18–22). However, the prognostic value of TLG in patients with NPC has not been sufficiently

Received Mar. 18, 2011; revision accepted Aug. 17, 2011.

For correspondence or reprints contact either of the following: Tzu-Chen Yen, Department of Nuclear Medicine and Molecular Imaging Center, Chang Gung Memorial Hospital, Chang Gung University College of Medicine, 199 Tung Hwa North Rd., Taipei, Taiwan 105.

E-mail: yen1110@cgmh.org.tw

Kai-Ping Chang, Department of Otolaryngology-Head & Neck Surgery, Chang Gung Memorial Hospital, Chang Gung University College of Medicine, 199 Tung Hwa North Rd., Taipei, Taiwan 105.

E-mail: changkp@cgmh.org.tw

COPYRIGHT © 2012 by the Society of Nuclear Medicine, Inc.

evaluated. In addition, whereas EBV DNA levels are associated with tumor volume quantified by MRI (23), data on the relationship between viral load and ^{18}F -FDG PET functional parameters are scarce (24).

In this study, we sought to examine the association of ^{18}F -FDG PET functional parameters and EBV DNA load with the clinicopathologic characteristics and clinical outcomes of patients with NPC. The combined use of blood-borne biomarkers and imaging parameters may eventually provide an individually tailored approach to the treatment of NPC.

MATERIALS AND METHODS

Study Patients

Informed consent was obtained from all participants, and the study protocol was approved by the Hospital Ethics Committee. The study population consisted of 108 patients with newly diagnosed NPC who were consecutively recruited at Chang Gung Memorial Hospital, Lin-Kou, Taiwan, between January 2006 and August 2009. Patients with metastatic disease at presentation (M1 stage), with other malignancies, or who had been previously treated at other institutions were excluded.

The study participants were staged with the 2002 cancer staging system revised by the American Joint Committee on Cancer (25). All patients had biopsy-proven NPC and received a thorough examination before therapy and every 6 mo after treatment. In brief, the examinations included head and neck MRI, chest radiography, and abdominal ultrasound. Before treatment, all participants underwent ^{18}F -FDG PET to confirm the initial clinical stage.

All patients received external-beam definitive radiotherapy for a cumulative dose of 64.8 Gy or higher. In keeping with our current treatment policy, all patients whose overall stage were 3 or greater received additional cisplatin-based concurrent chemoradiotherapy (1,2). Patients were followed every week during treatment and then every 3 mo for 2 y, every 4 mo for the next 2 y, and every 6 mo thereafter. Flexible fiberoptic nasopharyngoscopy was performed at each visit. A conventional work-up was performed 3 mo after completion of treatment and subsequently on a yearly basis or whenever clinically indicated.

The findings from ^{18}F -FDG PET and MRI were discussed jointly by our NPC research team. When possible, imaging-guided biopsies were obtained for lesions suggestive of malignancy. If a biopsy of the lesion of interest was not feasible or yielded a negative result in patients with equivocal or positive imaging results, close clinical and imaging follow-up was pursued. Patients with residual tumors confined to the primary site of origin were classified as having local failure. Patients with residual tumors in the neck lymph nodes were classified as having regional failure. Patients with disease beyond the primary lesion and regional lymph nodes were classified as having distant failure.

Collection and Storage of Blood Plasma

Before treatment, blood samples (10 mL) were collected through venipuncture in tubes containing ethylenediaminetetraacetic acid. Immediately after collection, samples were centrifuged (2,000g) to obtain the separated plasma and were then stored in polypropylene tubes at -80°C until analysis. Samples were not exposed to more than 1 freeze-thaw cycle.

Quantitation of Plasma EBV DNA Load

DNA extraction and quantification of plasma EBV DNA load were performed as described previously (11,26,27).

Imaging with ^{18}F -FDG PET/CT

All patients fasted for at least 6 h before ^{18}F -FDG PET/CT. Imaging was performed with a PET/CT system (Discovery ST 16; GE Healthcare) consisting of a PET scanner and a 16-section CT scanner. Before acquisition of PET images, helical CT was performed from the head to the proximal thigh according to a standardized protocol with the following settings: transverse 3.0-mm collimation \times 16 modes, 100 kVp, 100 mAs, 0.5-s tube rotation, 35-mm/s table speed, and pitch of 1.5. No intravenous iodinated contrast agents were administered. CT data were resized from a 512×512 matrix to a 128×128 matrix to match the PET data to fuse images and generate CT-based transmission maps. Emission scans from the head to the proximal thigh were acquired at 50–70 min after injection of 370 MBq of ^{18}F -FDG. Images were acquired in 2-dimensional mode, 3 min per table position. PET images were reconstructed with CT used for attenuation correction and an ordered-subset expectation maximization iterative reconstruction algorithm (4 iterations and 10 subsets).

Image Analysis

Semiquantitative evaluation was performed with a Syngo MI Workplace (Siemens Healthcare). The SUVs were determined by the region-of-interest technique. The maximum SUVs (SUVmax) were obtained by drawing the regions of interest over the most intense slice of the primary tumor within the nasopharynx and the neck lymph nodes. The value was calculated as follows: $\text{SUV} = (\text{decay-corrected activity [kBq]} \text{ per milliliter of tissue volume}) / (\text{injected } ^{18}\text{F}\text{-FDG activity [kBq]} / \text{body weight in grams})$.

The MTV was measured from attenuation-corrected ^{18}F -FDG PET images. The boundaries were drawn so as to include the primary tumor within the nasopharynx or metastatic regional lymph nodes in the axial, coronal, and sagittal ^{18}F -FDG PET/CT images. To define the contouring margins around the target, an SUV of 2.5 was used. The contour around the target lesion inside the boundaries was automatically produced, and the voxels presenting SUV intensity greater than 2.5 within the contouring margin were incorporated to define the MTV. The TLG was calculated according to the following formula: $\text{TLG} = \text{mean SUV} \times \text{MTV}$ (17).

The TLG values of the primary tumor, cervical lymph nodes, and total tumor (defined as the sum of the signal intensities of the primary tumor plus the cervical lymph nodes) were designated as tumor TLG, nodal TLG, and total TLG, respectively. The SUVmax of the primary tumor and the cervical lymph nodes were termed tumor SUVmax and nodal SUVmax, respectively.

Validation of Measurement of ^{18}F -FDG PET/CT Parameters

To validate all measured ^{18}F -FDG PET/CT parameters, all values were processed using PET VCAR (volume computer-assisted reading) software on an Advantage Workstation (GE Healthcare). A fixed SUV threshold of 2.5 was applied as the lowest limit of the automatic segmentation criteria. The bounding box used for selecting the volume of interest was placed and checked on 3 sectional PET images (axial, coronal, and sagittal) to ensure that the entire lesion was entirely included in the 3 dimensions. The single-component modality was deselected to prevent the segmentation that may potentially derive from grabbing normal structures

TABLE 1
General Characteristics of Study Participants

Characteristic	<i>n</i>
Sex	
Male	84 (77.7)
Female	24 (22.3)
Histologic type	
Squamous cell carcinoma	4 (3.7)
Nonkeratinizing carcinoma	39 (36.4)
Undifferentiated carcinoma	63 (58.1)
Other	2 (1.8)
T stage*	
T1	23 (21.2)
T2	30 (27.8)
T3	24 (22.2)
T4	30 (27.8)
N stage*	
N0	16 (14.8)
N1	39 (36.1)
N2	37 (34.3)
N3	15 (13.8)
Overall TNM stage*	
Stage I	6 (5.5)
Stage II	23 (21.3)
Stage III	34 (31.5)
Stage IV	44 (40.7)
EBV copy number (mL ⁻¹)	
Mean ± SD	3,502 ± 10,764
Total	108

*Data on TNM stage were lacking for 1 patient.

Mean age ± SD was 50.7 ± 14.3 y. Data in parentheses are percentages.

outside the volume of interest into the final calculation. The measurements of SUVmax, mean SUV, MTV, and TLG were uploaded automatically by the PET VCAR system.

Data Analysis

Continuous variables are presented as mean and SD. The correlation between PET parameters and plasma EBV DNA load was calculated by linear regression for continuous variables. All patients were followed until death or until December 2010. Univariate survival analyses were performed with the Kaplan–Meier method (log-rank test). The Cox proportional hazards regression model was used for multivariate analyses of the independent predictors for the rates of OS, DFS, local recurrence-free survival (LRFS), neck recurrence-free survival (NRFS), and distant metastasis-free survival (DMFS). All tests were 2-sided, and *P* values less than 0.05 were considered statistically significant.

RESULTS

Patient Characteristics

The general characteristics of the study participants are summarized in Table 1. At the time of the last follow-up, 88 patients were alive and 14 were dead. Thirty-one patients had tumor relapses after treatment. Sites of failure were as follows: local failure alone (*n* = 5), neck failure alone (*n* = 3), distant failure alone (*n* = 11), local and neck failure (*n* = 1), local and distant failure (*n* = 8), and neck and distant failure (*n* = 3) (Fig. 1).

Validation of Measurement of ¹⁸F-FDG PET/CT Parameters

All measured values of ¹⁸F-FDG PET/CT parameters derived from 2 different systems (Syngo MI Workplace and PET VCAR) were analyzed. The results indicated a marked degree of correlation between the 2 different measurement systems for all ¹⁸F-FDG PET parameters, including tumor TLG ($R^2 = 0.996$, $P < 0.0001$), nodal TLG ($R^2 = 0.998$, $P < 0.0001$), total TLG ($R^2 = 0.997$, $P < 0.0001$), tumor SUVmax ($R^2 = 0.998$, $P < 0.0001$), and nodal SUVmax ($R^2 = 0.999$, $P < 0.0001$).

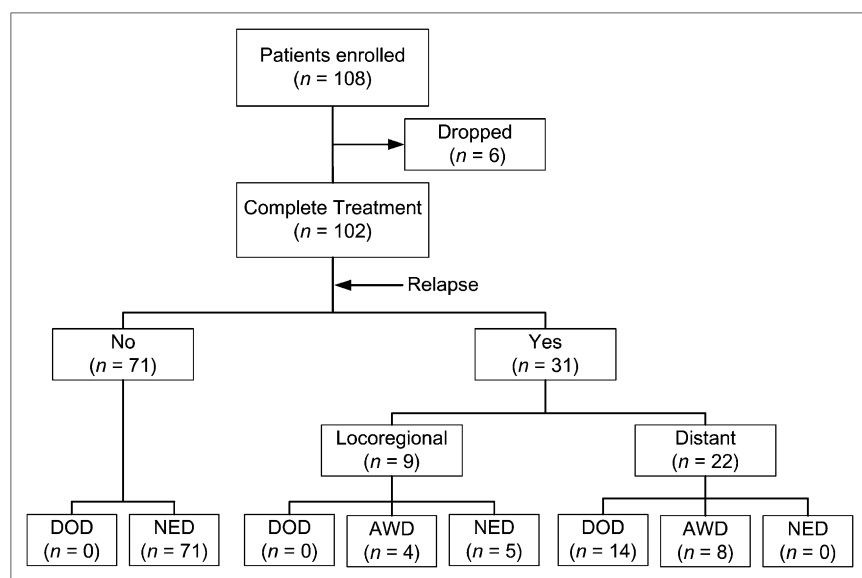


FIGURE 1. Flowchart of NPC patients throughout study (*n* = 108). AWD = alive with disease; DOD = die of disease; NED = no evidence of disease.

TABLE 2
Correlation Analyses of ^{18}F -FDG PET Functional Parameters and EBV DNA Copy Number (mL^{-1}) for Untreated NPC Patients

Parameter	Tumor TLG ($\text{g/mL} \times \text{mL}$)	Nodal TLG ($\text{g/mL} \times \text{mL}$)	Total TLG ($\text{g/mL} \times \text{mL}$)	Tumor SUVmax (g/mL)	Nodal SUVmax (g/mL)
R^2	0.251	0.447	0.589	0.199	0.462

Total TLG value was calculated as sum of primary tumor TLG and nodal TLG.

Association Between EBV DNA Load and ^{18}F -FDG PET Parameters

Linear regression analysis revealed the potential association between EBV DNA load and all ^{18}F -FDG PET parameters, including tumor TLG ($R^2 = 0.251$), nodal TLG ($R^2 = 0.447$), total TLG ($R^2 = 0.589$), tumor SUVmax ($R^2 = 0.199$), and nodal SUVmax ($R^2 = 0.462$, Table 2). The results indicated only total TLG was significantly correlated with EBV load.

Clinicopathologic Characteristics, ^{18}F -FDG PET Parameters, and EBV DNA Load

As shown in Table 3, higher T stages were associated with increased tumor TLG, total TLG, tumor SUVmax, and EBV DNA load. Compared with patients with N0 or N1 disease, those with N2 or N3 disease had higher nodal TLG,

total TLG, nodal SUVmax, and EBV DNA load. Similarly, patients with advanced NPC (stage III or IV) had higher tumor TLG, nodal TLG, total TLG, nodal SUVmax, and EBV DNA load than those with early disease (stage I or II). We did not find any significant association of ^{18}F -FDG PET parameters with age, sex, or the pathologic classification (Table 3).

^{18}F -FDG PET Parameters, EBV DNA Load, and Treatment Outcomes

Of the 108 study participants, 102 had complete standard treatment and routine follow-ups. These patients were divided into 2 equal groups ($n = 51$ each) on the basis of the median values of each ^{18}F -FDG PET parameter and EBV DNA load. As shown in Figure 2, Kaplan–Meier survival curves for OS did not differ significantly when

TABLE 3
Association of ^{18}F -FDG PET Functional Parameters and EBV DNA Copy Number with Clinicopathologic Characteristics of NPC Patients

Characteristic	<i>n</i>	Tumor		Nodal		Total		Tumor		Nodal		EBV DNA	
		TLG (g/mL × mL)	<i>P</i>	TLG (g/mL × mL)	<i>P</i>	TLG (g/mL × mL)	<i>P</i>	SUVmax (g/mL)	<i>P</i>	SUVmax (g/mL)	<i>P</i>	Copy/mL	<i>P</i>
Sex													
Female	24	83 ± 93	0.226	70 ± 95	0.714	153 ± 122	0.100	11.1 ± 4.6	0.865	8.0 ± 5.4	0.681	2,786 ± 7,952	0.106
Male	84	161 ± 227		147 ± 322		308 ± 390		11.7 ± 6.3		9.2 ± 7.7		3,707 ± 1,1747	
Age (y)*													
<47.5	54	97 ± 107	0.227	143 ± 344	0.968	240 ± 365	0.220	11.3 ± 5.5	0.818	8.8 ± 7.2	0.827	2,264 ± 7,100	0.002
>47.5	54	190 ± 265		116 ± 222		307 ± 343		11.8 ± 6.3		9.0 ± 7.5		4,741 ± 13,431	
T stage†													
T1–T2	53	44 ± 46	<0.001	110 ± 207	0.848	155 ± 205	<0.001	10.0 ± 5.9	0.001	8.3 ± 7.2	0.531	2,270 ± 6,455	0.014
T3–T4	54	237 ± 254		147 ± 353		384 ± 428		13.0 ± 5.6		9.4 ± 7.5		4,761 ± 13,766	
N stage†													
N0–N1	55	137 ± 215	0.725	38 ± 70	<0.001	176 ± 215	0.001	11.7 ± 6.4	0.883	6.3 ± 6.1	<0.001	3,289 ± 12,897	0.026
N2–N3	52	146 ± 199		224 ± 389		370 ± 438		11.3 ± 5.4		11.6 ± 7.5		3,779 ± 8,199	
Overall stage†													
I–II	29	48 ± 53	<0.001	42 ± 75	0.002	91 ± 81	<0.001	11.0 ± 7.3	0.337	5.4 ± 5.5	0.001	395 ± 819	0.001
III–IV	78	176 ± 231		160 ± 331		337 ± 392		11.7 ± 5.4		10.2 ± 7.5		4,692 ± 12,474	
World Health Organization‡													
I	4	114 ± 170		115 ± 125		230 ± 140		10.6 ± 3.9		11.0 ± 4.4		1,069 ± 950	
II	39	177 ± 209	0.247	161 ± 386	0.750	338 ± 432	0.080	13.1 ± 6.4	0.067	9.5 ± 8.3	0.776	4,563 ± 14,590	0.246
III	63	127 ± 212		115 ± 226		243 ± 313		10.1 ± 4.3		8.5 ± 6.9		3,079 ± 8,299	
Other	2	115 ± 39		26 ± 36		141 ± 2.4		26.5 ± 19.6		4.9 ± 7.0		2,513 ± 3,532	

*Median value.

†Data on TNM stage were lacking for 1 patient.

‡World Health Organization II vs. III.

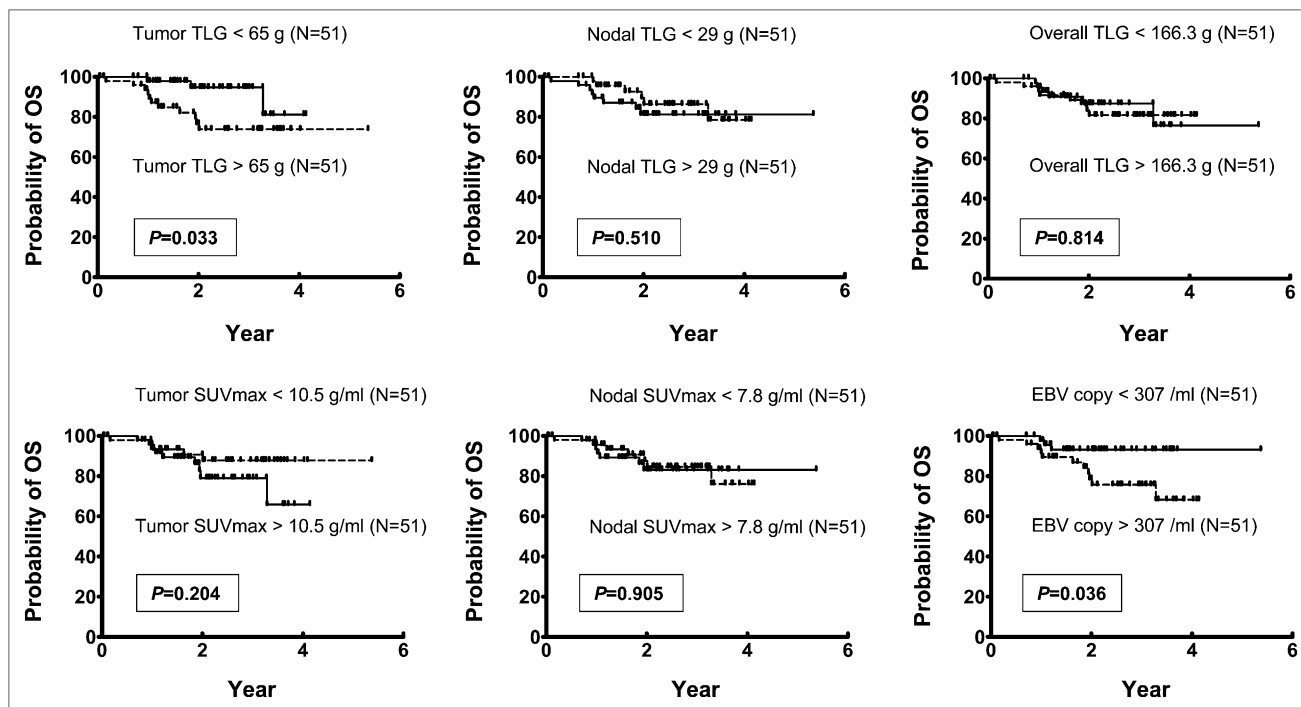


FIGURE 2. Kaplan–Meier estimates of OS rates for patients with NPC stratified according to median values of distinct ^{18}F -FDG PET functional parameters and EBV DNA load. Statistically significant differences by log-rank test are given.

patients were stratified according to the median value of nodal TLG, total TLG, tumor SUVmax, and nodal SUVmax. However, patients with higher values of tumor TLG and EBV DNA load had a significantly poorer OS ($P = 0.033$ and 0.036 , respectively), although the longest follow-up period for higher tumor TLG subgroup was only 4.13 y. Tumor TLG was the only parameter statistically significantly associated with LRFS ($P = 0.014$). Compared

with patients who had a tumor TLG less than 65 g (LRFS, 88.0%), those with tumor TLG greater than the median had an LRFS of 66.2%. Kaplan–Meier survival curves for NRFS did not differ significantly when patients were stratified according to the median value of all ^{18}F -FDG PET parameters and EBV DNA load (data not shown). As shown in Figure 3, tumor TLG was the only parameter significantly associated with DFS ($P < 0.001$). Compared with

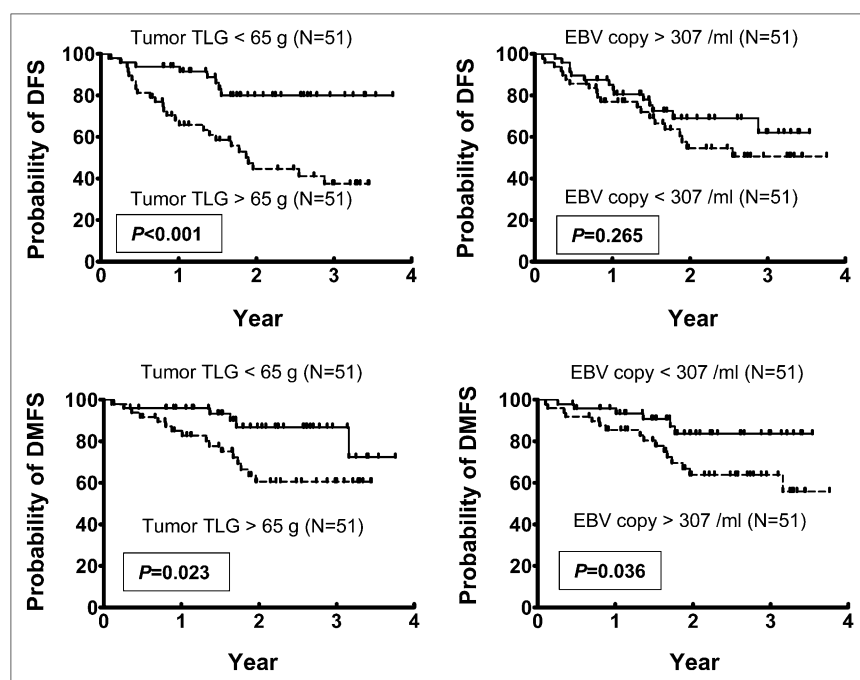


FIGURE 3. Kaplan–Meier estimates of DFS and DMFS rates for patients with NPC stratified according to median values of TLG measurement by ^{18}F -FDG PET and EBV DNA load. Statistically significant differences by log-rank test are given.

patients who had a tumor TLG less than 65 g (DFS, 79.9%), those with TLG greater than the median had a DFS of 37.4%. Kaplan–Meier survival curves for DMFS did not differ significantly when patients were stratified according to the median value of nodal TLG, total TLG, tumor SUVmax, and nodal SUVmax. However, as shown in Figure 3, tumor TLG and EBV DNA load were significantly associated with DMFS ($P = 0.023$ and 0.036 , respectively). Compared with patients who had a tumor TLG less than 65 g (DMFS, 72.3%), those with a tumor TLG greater than the median had a DMFS of 60.5%. In addition, patients with an EBV DNA load less than 307/mL (DMFS, 83.7%) had a better DMFS than those with an EBV DNA load greater than the median (DMFS, 55.8%). Furthermore, when we stratified the patients by both tumor TLG and EBV DNA load, we found that the patients with higher levels of both tumor TLG and EBV DNA load had significantly worse prognosis in OS, DFS, and DMFS ($P = 0.007$, 0.015 , and 0.012 , respectively) but not in LRFS and NRFS ($P = 0.082$ and 0.505 , respectively).

To determine whether various ^{18}F -FDG PET parameters and EBV DNA load can be used as independent predictors of different outcomes, we conducted a multivariate analysis of OS, LRFS, NRFS, DFS, and DMFS with Cox proportional regression models. Adjustment was also performed for age at onset, sex, and overall clinical stage. Our results indicated that higher values of tumor TLG ($P = 0.045$) and EBV DNA load ($P = 0.035$) retained their independent prognostic significance for poorer OS. Cox regression analysis also showed that a higher value of tumor TLG was also an independent prognostic factor for poorer DFS ($P = 0.006$, Fig. 4).

DISCUSSION

Evidence suggests that plasma EBV DNA is a prognostic marker in NPC patients, but its clinical utility has not been fully established (28–32). Our previous studies have also indicated the value of serum levels of MIP-3 α , cystatin A, vascular endothelial growth factor, and IL-8 for predicting outcomes in this malignancy (26,27,33). In addition, we have recently shown that the plasma EBV DNA copy number was significantly correlated with concentrations of these blood markers, further strengthening the concept that EBV DNA load is the core biomarker in the setting of NPC tumorigenesis (27). Notably, Ma et al. have recently reported

that the level of circulating EBV DNA was significantly associated with NPC tumor volume as assessed by MRI as well as SUV of the primary tumor and the metastatic lymph nodes (23), but they did not demonstrate the measurement of other ^{18}F -FDG PET functional parameters. Wang et al. addressed the potential utility of posttreated plasma EBV DNA and ^{18}F -FDG PET in detecting tumor relapse after treatment, but they did not evaluate any pretreated measurement of EBV DNA load and ^{18}F -FDG PET as described in the current study (34).

We have previously shown that ^{18}F -FDG PET is more sensitive than skeletal scintigraphy for the detection of bone metastases in patients with NPC at the initial staging (16). In addition, ^{18}F -FDG PET is superior to MRI for identifying lower neck nodal metastases from NPC before treatment (35,36) and ensures an improved detection of tumor relapse in the primary site, cervical lymph nodes, and distant sites after treatment (15,36–38). For these reasons, ^{18}F -FDG PET is increasingly used in the clinical staging, treatment planning, and monitoring of patients with NPC. Although evaluation of SUVmax by ^{18}F -FDG PET has been shown to predict prognosis after treatment of NPC (39), the relationships between different ^{18}F -FDG PET functional parameters and EBV DNA load has not been described before. The results from this study suggest that tumor TLG, nodal TLG, total TLG, tumor SUVmax, and nodal SUVmax were all significantly associated with plasma EBV DNA load. The highest degree of correlation was obtained between total TLG and EBV DNA load, suggesting a close association between this blood biomarker and the MTV and activity as assessed by ^{18}F -FDG PET.

We found that an association existed between tumor TLG and SUVmax with more advanced tumor stages as assessed by MRI. Similarly, nodal TLG values and SUVmax were found to be related to more advanced nodal stages. However, only total TLG and EBV DNA load were consistently and significantly associated with tumor, nodal, and overall clinical stages. Taken together, these results indicate that total TLG as assessed by PET in patients with NPC is closely associated with TNM stages as defined by MRI. In addition, the current study shows that there were no differences between the pathologic classifications of NPC tumors and the MTV and activity as quantified by various functional ^{18}F -FDG PET parameters. In keeping

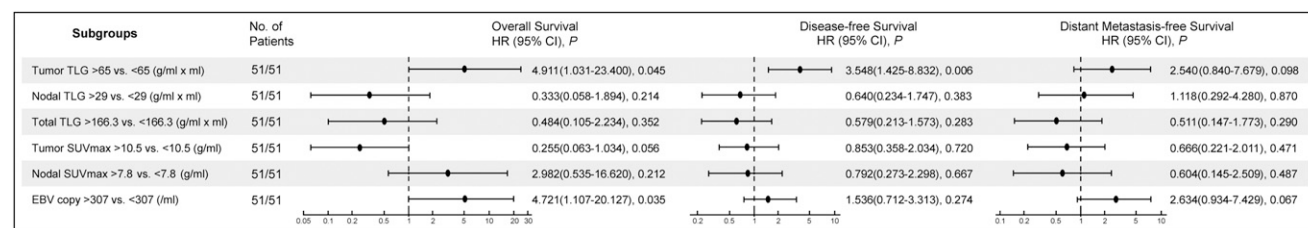


FIGURE 4. Multivariate Cox regression analyses of OS, DFS, and DMFS for patients with NPC stratified according to median values of distinct ^{18}F -FDG PET functional parameters and EBV DNA load. Multivariate model included age, sex, overall stage, tumor TLG, nodal TLG, total TLG, tumor SUVmax, nodal SUVmax, and EBV DNA load as covariates. Results showed that tumor TLG values and EBV DNA load were independent predictors of OS, whereas tumor TLG independently predicted DFS. CI = confidence interval; HR = hazard ratio.

with previous data (12,13,26,27,40), this study confirms the prognostic value of baseline EBV DNA load for predicting OS. We also found that tumor TLG values were higher than the median predicted poor rates of OS, LRFS, DFS, and DMFS by univariate analysis, and they were independently associated with OS and DFS after multivariate Cox regression analysis. These findings suggest that pretreatment primary tumor TLG values may be used to predict the prognosis of NPC treatment, whereas total TLG had the highest degree of correlation with EBV DNA load and TNM clinical stages. This apparent discrepancy may be explained, at least in part, by the fact that tumor relapse in the cervical lymph nodes is relatively unusual after current NPC treatment, compared with relapses at either primary or distant sites (41,42). In addition, relapse at the cervical lymph nodes can be generally managed by salvage surgery (e.g., with radical neck dissection) (6). In this context, the adverse prognostic impact of nodal recurrence is generally lower than that of tumor or distant relapse. This may also account for the observation that nodal TLG, nodal SUVmax, and even total TLG (which partially depends on nodal TLG values) did not predict certain survival endpoints.

CONCLUSION

This study conducted in patients with NPC suggests that total TLG values are mainly associated with tumor burden and clinical stage, whereas tumor TLG is the best predictor of rates of OS, DFS, and DMFS after treatment. These findings provide additional evidence supporting the use of ^{18}F -FDG PET in the clinical management of patients with NPC. Further studies are needed to clarify whether the combined assessment of ^{18}F -FDG PET functional parameters and EBV DNA level can improve patient outcomes through an optimized biomarker-guided and imaging-guided treatment strategy.

DISCLOSURE STATEMENT

The costs of publication of this article were defrayed in part by the payment of page charges. Therefore, and solely to indicate this fact, this article is hereby marked "advertisement" in accordance with 18 USC section 1734.

ACKNOWLEDGMENTS

This study was supported by grants NSC99-2314-B-182A-034-MY3 from the National Science Council; DOH99-TD-C-111-006 from the Department of Health; and CMRPG390641 and CMRPG390642 from Chang Gung University and Chang Gung Memorial Hospital, Taiwan. No other potential conflict of interest relevant to this article was reported.

REFERENCES

- Cheng SH, Jian JJ, Tsai SY, et al. Long-term survival of nasopharyngeal carcinoma following concomitant radiotherapy and chemotherapy. *Int J Radiat Oncol Biol Phys*. 2000;48:1323–1330.
- Lin JC, Jan JS, Hsu CY, Liang WM, Jiang RS, Wang WY. Phase III study of concurrent chemoradiotherapy versus radiotherapy alone for advanced nasopharyngeal carcinoma: positive effect on overall and progression-free survival. *J Clin Oncol*. 2003;21:631–637.
- Chan AT, Teo PM, Ngan RK, et al. Concurrent chemotherapy-radiotherapy compared with radiotherapy alone in locoregionally advanced nasopharyngeal carcinoma: progression-free survival analysis of a phase III randomized trial. *J Clin Oncol*. 2002;20:2038–2044.
- Chang KP, Hao SP, Tsang NM, Ueng SH. Salvage surgery for locally recurrent nasopharyngeal carcinoma: a 10-year experience. *Otolaryngol Head Neck Surg*. 2004;131:497–502.
- Wei WI, Chan JY, Ng RW, Ho WK. Surgical salvage of persistent or recurrent nasopharyngeal carcinoma with maxillary swing approach: critical appraisal after 2 decades. *Head Neck*. 2011;33:969–975.
- Wei WI, Lam KH, Ho CM, Sham JS, Lau SK. Efficacy of radical neck dissection for the control of cervical metastasis after radiotherapy for nasopharyngeal carcinoma. *Am J Surg*. 1990;160:439–442.
- Chang YS, Tyan YS, Liu ST, Tsai MS, Pao CC. Detection of Epstein-Barr virus DNA sequences in nasopharyngeal carcinoma cells by enzymatic DNA amplification. *J Clin Microbiol*. 1990;28:2398–2402.
- Raab-Traub N. Epstein-Barr virus and nasopharyngeal carcinoma. *Semin Cancer Biol*. 1992;3:297–307.
- Wu TC, Mann RB, Epstein JI, et al. Abundant expression of EBER1 small nuclear RNA in nasopharyngeal carcinoma: a morphologically distinctive target for detection of Epstein-Barr virus in formalin-fixed paraffin-embedded carcinoma specimens. *Am J Pathol*. 1991;138:1461–1469.
- Henle G, Henle W. Epstein-Barr virus-specific IgA serum antibodies as an outstanding feature of nasopharyngeal carcinoma. *Int J Cancer*. 1976;17:1–7.
- Lo YM, Chan LY, Lo KW, et al. Quantitative analysis of cell-free Epstein-Barr virus DNA in plasma of patients with nasopharyngeal carcinoma. *Cancer Res*. 1999;59:1188–1191.
- Chang KP, Hsu CL, Chang YL, et al. Complementary serum test of antibodies to Epstein-Barr virus nuclear antigen-1 and early antigen: a possible alternative for primary screening of nasopharyngeal carcinoma. *Oral Oncol*. 2008;44:784–792.
- Lin JC, Wang WY, Chen KY, et al. Quantification of plasma Epstein-Barr virus DNA in patients with advanced nasopharyngeal carcinoma. *N Engl J Med*. 2004;350:2461–2470.
- Yen TC, Chang YC, Chan SC, et al. Are dual-phase ^{18}F -FDG PET scans necessary in nasopharyngeal carcinoma to assess the primary tumour and locoregional nodes? *Eur J Nucl Med Mol Imaging*. 2005;32:541–548.
- Chan SC, Yen TC, Ng SH, et al. Differential roles of ^{18}F -FDG PET in patients with locoregional advanced nasopharyngeal carcinoma after primary curative therapy: response evaluation and impact on management. *J Nucl Med*. 2006;47:1447–1454.
- Liu FY, Chang JT, Wang HM, et al. [^{18}F]fluorodeoxyglucose positron emission tomography is more sensitive than skeletal scintigraphy for detecting bone metastasis in endemic nasopharyngeal carcinoma at initial staging. *J Clin Oncol*. 2006;24:599–604.
- Larson SM, Erdi Y, Akhurst T, et al. Tumor treatment response based on visual and quantitative changes in global tumor glycolysis using PET-FDG imaging: the visual response score and the change in total lesion glycolysis. *Clin Positron Imaging*. 1999;2:159–171.
- Erdi YE, Macapinlac H, Rosenzweig KE, et al. Use of PET to monitor the response of lung cancer to radiation treatment. *Eur J Nucl Med*. 2000;27:861–866.
- Gu J, Khong PL, Wang S, Chan Q, Law W, Zhang J. Quantitative assessment of diffusion-weighted MR imaging in patients with primary rectal cancer: correlation with FDG-PET/CT. *Mol Imaging Biol*. 2010;12:25–34.
- Guillemin JG, Moore HG, Akhurst T, et al. Sequential preoperative fluorodeoxyglucose-positron emission tomography assessment of response to preoperative chemoradiation: a means for determining longterm outcomes of rectal cancer. *J Am Coll Surg*. 2004;199:1–7.
- Melton GB, Lavelly WC, Jacene HA, et al. Efficacy of preoperative combined ^{18}F -fluorodeoxyglucose positron emission tomography and computed tomography for assessing primary rectal cancer response to neoadjuvant therapy. *J Gastrointest Surg*. 2007;11:961–969.
- Tateishi U, Gamez C, Dawood S, Yeung HW, Cristofanilli M, Macapinlac HA. Bone metastases in patients with metastatic breast cancer: morphologic and metabolic monitoring of response to systemic therapy with integrated PET/CT. *Radiology*. 2008;247:189–196.
- Ma BB, King A, Lo YM, et al. Relationship between pretreatment level of plasma Epstein-Barr virus DNA, tumor burden, and metabolic activity in advanced nasopharyngeal carcinoma. *Int J Radiat Oncol Biol Phys*. 2006;66:714–720.
- Mäkitie AA, Reis PP, Irish J, et al. Correlation of Epstein-Barr virus DNA in cell-free plasma, functional imaging and clinical course in locally advanced nasopharyngeal cancer: a pilot study. *Head Neck*. 2004;26:815–822.

25. O'Sullivan B, Shah J. New TNM staging criteria for head and neck tumors. *Semin Surg Oncol*. 2003;21:30–42.
26. Chang KP, Hao SP, Chang JH, et al. Macrophage inflammatory protein-3 α is a novel serum marker for nasopharyngeal carcinoma detection and prediction of treatment outcomes. *Clin Cancer Res*. 2008;14:6979–6987.
27. Chang KP, Chang YT, Wu CC, et al. Multiplexed immunobead-based profiling of cytokine markers for detection of nasopharyngeal carcinoma and prognosis of patient survival. *Head Neck*. 2011;33:886–897.
28. Cho WC, Yip TT, Yip C, et al. Identification of serum amyloid A protein as a potentially useful biomarker to monitor relapse of nasopharyngeal cancer by serum proteomic profiling. *Clin Cancer Res*. 2004;10:43–52.
29. Ho S, Leung WT, Yuen J, Johnson PJ. Serum levels of CYFRA 21-1 in nasopharyngeal carcinoma and its possible role in monitoring of therapy. *Eur J Cancer B Oral Oncol*. 1996;32B:377–380.
30. Xu J, Menezes J, Prasad U, Ahmad A. Elevated serum levels of transforming growth factor β 1 in Epstein-Barr virus-associated nasopharyngeal carcinoma patients. *Int J Cancer*. 1999;84:396–399.
31. Tan EL, Selvaratnam G, Kananathan R, Sam CK. Quantification of Epstein-Barr virus DNA load, interleukin-6, interleukin-10, transforming growth factor- β 1 and stem cell factor in plasma of patients with nasopharyngeal carcinoma. *BMC Cancer*. 2006;6:227.
32. Hui EP, Sung FL, Yu BK, et al. Plasma osteopontin, hypoxia, and response to radiotherapy in nasopharyngeal cancer. *Clin Cancer Res*. 2008;14:7080–7087.
33. Chang KP, Wu CC, Chen HC, et al. Identification of candidate nasopharyngeal carcinoma serum biomarkers by cancer cell secretome and tissue transcriptome analysis: potential usage of cystatin A for predicting nodal stage and poor prognosis. *Proteomics*. 2010;10:2644–2660.
34. Wang WY, Twu CW, Lin WY, et al. Plasma Epstein-Barr virus DNA screening followed by ^{18}F -fluoro-2-deoxy-D-glucose positron emission tomography in detecting posttreatment failures of nasopharyngeal carcinoma. *Cancer*. 2011;117:4452–4459.
35. Chang JT, Chan SC, Yen TC, et al. Nasopharyngeal carcinoma staging by ^{18}F -fluorodeoxyglucose positron emission tomography. *Int J Radiat Oncol Biol Phys*. 2005;62:501–507.
36. Ng SH, Chan SC, Yen TC, et al. Staging of untreated nasopharyngeal carcinoma with PET/CT: comparison with conventional imaging work-up. *Eur J Nucl Med Mol Imaging*. 2009;36:12–22.
37. Chan SC, Chang JT, Wang HM, et al. Prediction for distant failure in patients with stage M0 nasopharyngeal carcinoma: the role of standardized uptake value. *Oral Oncol*. 2009;45:52–58.
38. Chan SC, Ng SH, Chang JT, et al. Advantages and pitfalls of ^{18}F -fluoro-2-deoxy-D-glucose positron emission tomography in detecting locally residual or recurrent nasopharyngeal carcinoma: comparison with magnetic resonance imaging. *Eur J Nucl Med Mol Imaging*. 2006;33:1032–1040.
39. Xie P, Yue JB, Fu Z, Feng R, Yu JM. Prognostic value of ^{18}F -FDG PET/CT before and after radiotherapy for locally advanced nasopharyngeal carcinoma. *Ann Oncol*. 2010;21:1078–1082.
40. Leung SF, Zee B, Ma BB, et al. Plasma Epstein-Barr viral deoxyribonucleic acid quantitation complements tumor-node-metastasis staging prognostication in nasopharyngeal carcinoma. *J Clin Oncol*. 2006;24:5414–5418.
41. Lee AW, Poon YF, Foo W, et al. Retrospective analysis of 5037 patients with nasopharyngeal carcinoma treated during 1976–1985: overall survival and patterns of failure. *Int J Radiat Oncol Biol Phys*. 1992;23:261–270.
42. Chang KP, Hao SP, Lin SY, et al. The 30-bp deletion of Epstein-Barr virus latent membrane protein-1 gene has no effect in nasopharyngeal carcinoma. *Laryngoscope*. 2006;116:541–546.



The Journal of
NUCLEAR MEDICINE

Prognostic Significance of ^{18}F -FDG PET Parameters and Plasma Epstein-Barr Virus DNA Load in Patients with Nasopharyngeal Carcinoma

Kai-Ping Chang, Ngan-Ming Tsang, Chun-Ta Liao, Cheng-Lung Hsu, Ming-Jui Chung, Chuan-Wei Lo, Sheng-Chieh Chan, Shu-Hang Ng, Hung-Ming Wang and Tzu-Chen Yen

J Nucl Med. 2012;53:21-28.

Doi: 10.2967/jnumed.111.090696

This article and updated information are available at:
<http://jnm.snmjournals.org/content/53/1/21>

Information about reproducing figures, tables, or other portions of this article can be found online at:
<http://jnm.snmjournals.org/site/misc/permission.xhtml>

Information about subscriptions to JNM can be found at:
<http://jnm.snmjournals.org/site/subscriptions/online.xhtml>

The Journal of Nuclear Medicine is published monthly.
SNMMI | Society of Nuclear Medicine and Molecular Imaging
1850 Samuel Morse Drive, Reston, VA 20190.
(Print ISSN: 0161-5505, Online ISSN: 2159-662X)

© Copyright 2012 SNMMI; all rights reserved.